

Ni-rich Nitrides ANNi₃ (A = Pt, Ag, Pd) in Comparison with Superconducting ZnNNi₃

M. A. Ali, A. K. M. A. Islam*, and M. S. Ali

Department of Physics, Rajshahi University

Received 26 November 2011, accepted 20 December 2011

Abstract

This article reports on the elastic, electronic and optical properties of predicted Ni-rich nitrides ANNi₃ (A = Pt, Ag, Pd) in comparison with isostructural superconducting counterpart ZnNNi₃. We have used first-principles density functional theory (DFT) with generalized gradient approximation (GGA). The independent elastic constants (C_{11} , C_{12} , and C_{44}), bulk modulus B , compressibility K , shear modulus G , and Poisson's ratio ν , as well as the band structures, total and partial densities of states and finally the optical properties of ANNi₃ have been calculated. The results are then analyzed and compared with those of the superconducting ZnNNi₃. The electronic band structures of the three compounds show metallic behavior with a high density of states at the Fermi level in which Ni $3d$ states dominate just like the superconducting ZnNNi₃. Analysis of T_c expression using available parameter values suggests that the three compounds are less likely to be superconductors. Optical reflectivity spectra indicate that all the compounds have the potential to be used as a coating to remove solar heating.

Keywords: ANNi₃; *Ab initio* calculations; Elastic properties; Electronic band structure; Optical properties.

© 2012 JSR Publications. ISSN: 2070-0237 (Print); 2070-0245 (Online). All rights reserved.
doi:10.3329/jsr.v4i1.9026 J. Sci. Res. 4 (1), 1-10 (2012)

1. Introduction

The ternary nitrides or carbides with the general formula AXM₃ (A: divalent or trivalent element; X: carbon or nitrogen; and M: transition metal) have already been known for several decades [1-3]. For some time now, since the discovery of superconductivity near 8 K in MgCNi₃ [4], attention has been directed on the isostructural cubic anti-perovskites, with the general formula ACNi₃, where A is a group II or III element as possible compounds with not only high superconducting transition temperature, but other technologically important properties.

Recently, a new superconducting anti-perovskite ZnNNi₃ with $T_c \sim 3$ K, which belongs to this class of materials, but with carbon replaced by nitrogen was successfully

* Corresponding author: azi46@ru.ac.bd

synthesized [5] and some of its properties have been investigated. ZnNNi_3 is the first nitrogen-containing superconducting material in the Ni-based anti-perovskite series. In the light of the rigid-band picture, the discovery seems to be intriguing since ZnNNi_3 anti-perovskite can be considered as a one electron doped superconducting $\text{M}^{\text{II}}\text{CNi}_3$ phase, where the Fermi level should be located far from the Ni $3d$ peak, i.e., in the region of quite a low DOS, which is unfavorable for superconductivity (see [6]). Moreover recently, a new antiperovskite-like ternary nitride InNNi_3 was successfully synthesized. This material has one excess valence electron as compared with superconducting ZnNNi_3 and shows metallic behavior [7]. Hou [8] has reported that the ground state of InNNi_3 , which is the same as for other Ni-based ternary nitrides or carbides with a cubic anti-perovskite structure, is non-magnetic. Thus the discovery of superconductivity in ZnNNi_3 has given strong motivation to study the Ni-based anti-perovskite series. As a result a number of research workers [5-15] have either synthesized or characterized through band structure calculations of six anti-perovskite-type Ni-rich nitrides ANNi_3 ($A = \text{Zn, Cd, Mg, Al, Ga}$ and In). Further formability of six more nitrides ANNi_3 ($A = \text{Sn, Sb, Pd, Cu, Ag, Pt}$) have been empirically predicted [16]. Recently some mechanical properties of twelve MNNi_3 -type compounds with $A = \text{Zn, Mg, Cd, Al, Ga, In, Sn, Sb, Pd, Cu, Ag, Pt}$ have been examined theoretically [17]. Among the six predicted hypothetical compounds, only SnNNi_3 and CuNNi_3 have been subjected to first-principles investigations by Helal and Islam [18].

Thus despite a number of interesting results on physical properties for cubic Ni-rich nitrides ANNi_3 , which were reported in past years [5-18], no work has been done on the electronic and optical properties of the compounds PtNNi_3 , AgNNi_3 and PdNNi_3 . Therefore elastic properties, metallic behavior using band structure calculation and optical properties of these three Ni-rich materials in comparison with the superconducting ZnNNi_3 would reveal new information about the unexplored new materials.

2. Computational Method

The calculations were performed in the framework of density functional theory (DFT) [19] using generalized gradient approximations (GGA) with exchange-correlation potential due to Perdew, Burke and Ernzerhoff (GGA-PBE) [20] all of which are implemented in the CASTEP code [21]. Here periodic boundary conditions are utilized, and the electronic wave functions are expanded in a plane-wave basis set. In order to ensure convergence with respect to the basis set, the expansion includes all plane waves with kinetic energies less than a cut-off-energy. The ionic cores were represented by ultrasoft pseudopotentials for Ag, Pd, Pt, Zn, N, and Ni atoms. $5d^9$, $6s^1$ (Pt), $5s^1$ (Ag), $4d^{10}$ (Pd), $3d^{10}$, $4s^2$ (Zn), $2s^2$, $2p^3$ (N), and $3d^8$, $4s^2$ (Ni) electrons were treated as part of the valence states of the atoms. The plane-wave cutoff energy was 500 eV, and the Brillouin-zone integration was performed over the $15 \times 15 \times 15$ grid sizes using the Monkhorst-Pack [22] method for structural optimization. The structural parameters of ANNi_3 were determined using the BFGS [23] minimization technique.

3. Results and Discussion

3.1. Structural and elastic properties

ANNi₃ (A = Pt, Ag, Pd and Zn) belong to the cubic systems with space group Pm-3m (221) consisting A atoms at the corners, N at the body center and Ni at the face centers of the cube. The atomic positions are Ni: $3c$ ($\frac{1}{2}$, $\frac{1}{2}$, 0), A: $1a$ (0, 0, 0), and N: $1b$ ($\frac{1}{2}$, $\frac{1}{2}$, $\frac{1}{2}$). The total energy is minimized by the geometry optimization and the optimized values of structural parameters of ANNi₃ are shown in Table 1 along with other theoretical results. The obtained lattice parameters are in good agreement with the results obtained by Bannikov *et al.* [17]. The calculated independent elastic constants are also included in Table 1. For cubic systems the mechanical stability requires the elastic constants to satisfy the general criteria [24]: $(C_{11}-C_{12}) > 0$; $(C_{11} + 2C_{12}) > 0$; $C_{44} > 0$. These conditions also lead to a restriction on the value of the bulk modulus B , which is required to be in between C_{11} and C_{12} , i.e., $C_{12} < B < C_{11}$. From the table, we see that the independent elastic constants are all positive and satisfy the conditions of mechanical stability.

Table 1. The optimized structural parameters, independent elastic constants C_{ij} , bulk modulus B , compressibility K , shear modulus G , tetragonal shear modulus G' , Pugh ratio G/B , Young's modulus Y , Poisson ratio ν , Zenger's anisotropy index A of ANNi₃ (A = Pt, Ag, Pd and Zn).

Parameters	PtNNi ₃	AgNNi ₃	PdNNi ₃	ZnNNi ₃
a (Å)	3.821, 3.809 ^a	3.846, 3.832 ^a	3.809, 3.803 ^a	3.784, 3.770 ^a
C_{11} (GPa)	342.0, 316.9 ^a	307.2, 321.1 ^a	315.6, 313.3 ^a	335.62, 381.6 ^a
C_{12} (GPa)	170.4, 197.7 ^a	138.8, 130.0 ^a	168.3, 161.5 ^a	124.84, 116.5 ^a
C_{44} (GPa)	53.0, 50.5 ^a	44.2, 48.9 ^a	42.8, 81.1 ^a	48.43, 48.06 ^b
B (GPa)	227.6, 237.4 ^a	194.5, 193.7 ^a	217.4, 212.1 ^a	195.1, 204.9 ^a
K (GPa ⁻¹)	0.0043, 0.0042 ^a	0.0051, 0.0052 ^a	0.0046, 0.0047 ^a	0.0051, 0.0049 ^a
G (GPa)	64.4, 54.0 ^a	57.4, 64.1 ^a	55.3, 78.9 ^a	48.43, 48.06 ^b
G' (GPa)	176.5, 150.5 ^a	84.2, 95.5 ^a	73.6, 75.9 ^a	105.3, 132.5 ^a
Y (GPa)	176.5, 150.5 ^a	156.7, 173.3 ^a	152.9, 210.8 ^a	133.8, 127.4 ^a
ν	0.37, 0.39 ^a	0.36, 0.35 ^a	0.38, 0.33 ^a	0.34, 0.39 ^a
A	0.61, 0.84 ^a	0.52, 0.51 ^a	0.58, 1.06 ^a	0.45, 0.13 ^a
G/B	0.28, 0.22 ^a	0.29, 0.33 ^a	0.25, 0.37 ^a	0.24, 0.22 ^a

^aRef. [17]; ^bRef. [12].

The calculated elastic parameters (bulk moduli B , compressibility K , shear moduli G , Pough ratio, Young's moduli Y , the Poisson ratio ν and Zenger's anisotropy index, A) are given in Table 1. Y and ν are computed using the relationships: $Y = 9BG / (3B + G)$, $\nu = (3B - Y) / 6B$ [25]. The bulk modulus B and shear modulus G is obtained from elastic

constants according to the Voigt-Reuss-Hill (VRH) average scheme [26]. The subscript V denotes the Voigt bound, R denotes the Reuss bound. The arithmetic average of Voigt and Reuss bounds is termed as the Voigt-Reuss-Hill approximations [27] $B_H \equiv B = \frac{1}{2}(B_R + B_V)$ and $G_H \equiv G = \frac{1}{2}(G_R + G_V)$. The tetragonal shear moduli, $G' = (C_{11} - C_{12})/2$ and Zenger's anisotropy index, $A = 2C_{44}/(C_{11} - C_{12})$ [28] are calculated.

Now let us have a closer look at Table 1. Since the bulk modulus B describes the resistance of a material to volume change. We see that it is more difficult to change volume of PtNNi₃ than the other examined compounds. The bulk modulus of B (PtNNi₃) > B (PdNNi₃) > B (ZnNNi₃) > B (AgNNi₃) and the compressibility are in inverse order. Let us note also that for phases under consideration $B > G' > G$; this implies that the parameter limiting the mechanical stability of these materials are the shear modulus G . The Young's modulus Y is used often to denote a measure of stiffness. Among the phases in Table 1, PtNNi₃ is the stiffest and, PtNNi₃, AgNNi₃ and PdNNi₃ are stiffer than ZnNNi₃. As the Poisson's ratio for brittle material is small, whereas for ductile metallic material ν is typically 0.33 [29], we can see that the examined compounds show ductile metallic behavior. The deviations of Zenger's anisotropy from unity measure the degree of elastic anisotropy. Our results show that all the compounds under consideration are anisotropic and AgNNi₃, PdNNi₃ and PtNNi₃ are more anisotropic than ZnNNi₃. In order to predict the brittle and ductile behavior of solids, Pugh [30] gave a critical value for ductile-brittle transition. If $G/B > 0.5$, the material behaves in a brittle manner, otherwise, in a ductile manner. From Table 1, we see that PtNNi₃, AgNNi₃, PdNNi₃ and ZnNNi₃ are all ductile.

3.2. *Electronic properties*

The calculated energy band structures for PtNNi₃, AgNNi₃, PdNNi₃, and ZnNNi₃, at equilibrium lattice parameters, along the high symmetry directions in the Brillouin zone are shown in Fig. 1. The obtained band structures of (a) PtNNi₃ (b) AgNNi₃ and (c) PdNNi₃ are similar to those of ZnNNi₃ obtained by Helal and Islam [18]. The valence and conduction bands overlap considerably and there is no band gap at the Fermi level. As a result all the compounds under consideration exhibit metallic properties. To further elucidate the nature of conductivity in these compounds, we study the total and partial density of states (PDOS) of PtNNi₃, AgNNi₃, PdNNi₃, and ZnNNi₃ as shown in Fig. 2. At the Fermi level E_F , the DOS values for PtNNi₃, AgNNi₃, PdNNi₃ and ZnNNi₃ are 7.11, 5.20, 8.20 and 3.0, respectively. Concerning the atoms in the cell, the contribution of A (Pt, Ag, Pd, Zn), N and Ni atoms can clearly be seen. In fact the energy bands around the Fermi level are mainly from Ni 3d states, suggesting that Ni 3d states dominate the conductivity for each of the phases.

The DOS of ZnNNi₃ is the smallest of the four compounds, and it is a synthesized superconductor. In order to elucidate the possible occurrence of superconductivity in the other three compounds, investigation about electron-phonon coupling properties of the compound should be performed. McMillan's formula for T_c [31] is proportional to Debye temperature θ_D and an exponential term involving electron-phonon coupling constant, $\lambda =$

$N(E_F) \langle I^2 \rangle / M \langle \omega^2 \rangle$. Here M is the relevant atomic mass, $\langle I^2 \rangle$ the square of the e-phonon matrix element averaged over the Fermi surface, $\langle \omega^2 \rangle$ is the relevant phonon frequency squared, $N(E_F)$ is the DOS at the E_F . This may be invoked to infer superconductivity of the three new compounds [32]. It can be seen from the expression that DOS would affect T_c only if the $\langle I^2 \rangle$ is the same for all the three compounds. However A is different which would alter the e-ph coupling. All compounds have N, Ni in common. Only the masses of A-metals are different (mass in amu: 65.40 (Zn), 107.86 (Ag), 106.42 (Pd), 195.07 (Pt)), which will alter the electron-phonon coupling with the modified potential. Our calculated Debye temperatures θ_D (K) are: 357 (PtNNi₃), 381 (PdNNi₃), 392 (AgNNi₃), and 490 (ZnNNi₃). The T_c equation when analysed with all these factors indicates that the three compounds are less likely to be superconductors, or at best their T_c will be smaller than that of superconducting ZnNNi₃.

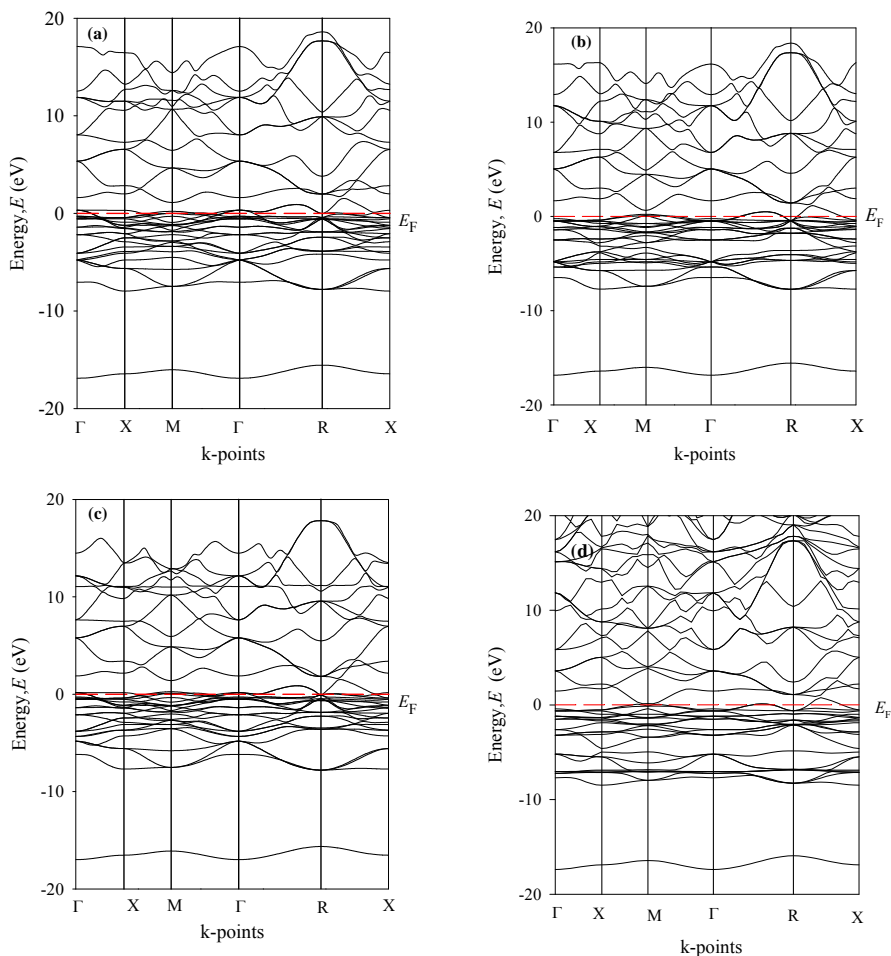


Fig. 1. Electronic band structure of (a) PtNNi₃, (b) AgNNi₃, (c) PdNNi₃ and (d) ZnNNi₃.

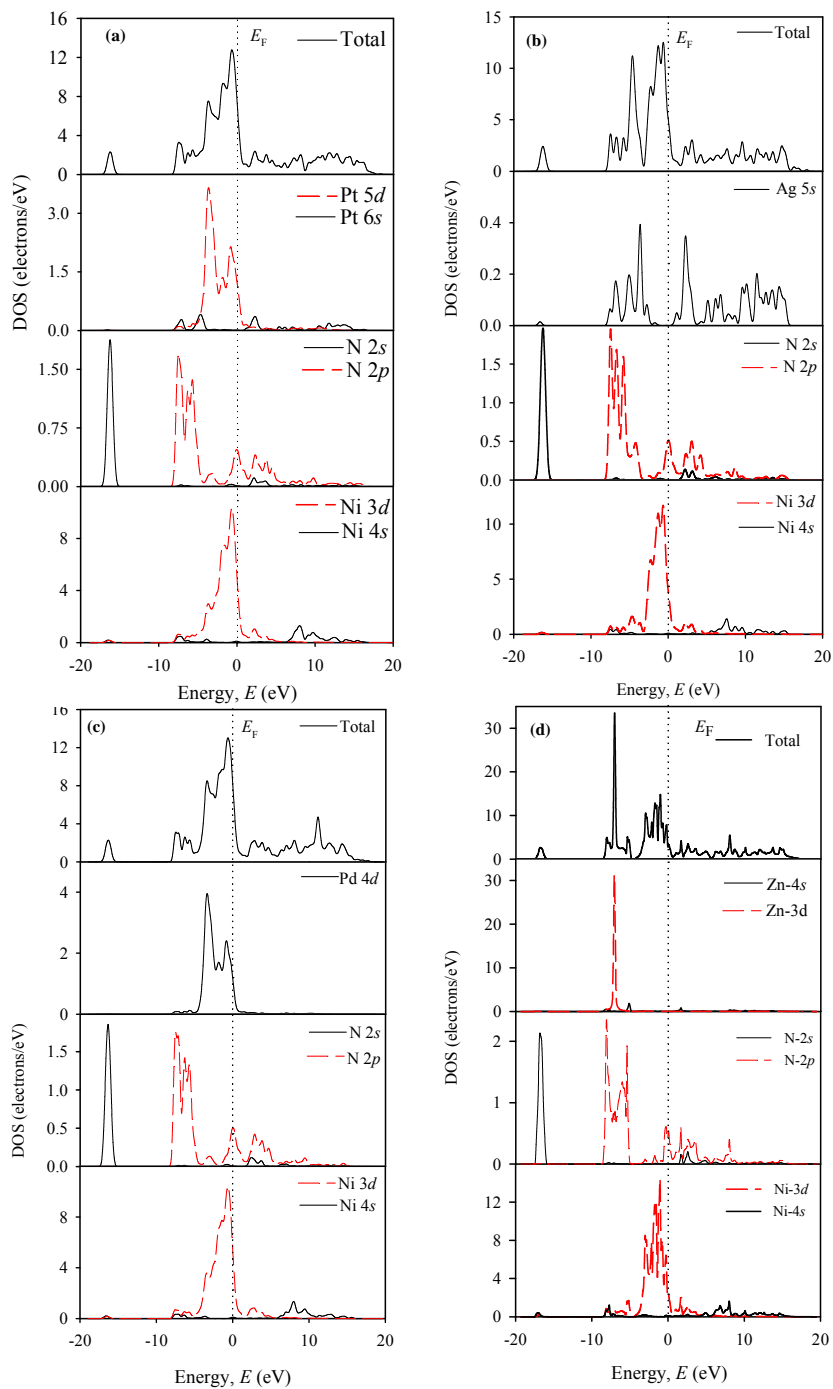


Fig. 2. Total and partial densities of states of (a) PtNNi₃, (b) AgNNi₃, (c) PdNNi₃, and (d) ZnNNi₃.

The lowest energy bands are mainly derived from N 2s for ANNi₃ (A = Pt, Ag, Pd and Zn). The energy bands between -10 to 0 eV are dominated by hybridizing Ni 3d and N 2p states. In the conduction band N 2p, Ni 4s dominates the energy bands.

3.3. Optical properties

Optical properties are directly related to the electronic properties. In order to get better insight of the electronic properties, the optical properties of ANNi₃ (A = Pt, Ag, and Pd) have been calculated for photon energy up to 30 eV and then compared with those of the ZnNNi₃ [18]. We have used a 0.5 eV Gaussian smearing for all calculations. This smears out the Fermi level, so that k-points will be more effective on the Fermi surface. The optical properties of ANNi₃ (A = Pt, Ag, and Pd) are similar to the ZnNNi₃ but not identical. There are differences in the position of the peaks.

The dielectric functions are shown in Fig. 3. The primary quantity that characterizes the electronic structure of any crystalline material is the probability of photon absorption, which is directly related to the imaginary part of the optical dielectric function $\epsilon(\omega)$. In the case of $\epsilon_2(\omega)$, There is only one peak for AgNNi₃, PdNNi₃ and ZnNNi₃ at 0.7, 0.19 and 0.36 eV respectively. There is no such peak for PtNNi₃. The high values of the static dielectric function for PtNNi₃, AgNNi₃, PdNNi₃, and ZnNNi₃ indicate that these compounds are promising dielectric materials.

We also observed that the calculated absorption coefficient in Fig. 4(a) and optical conductivity in Fig. 4(b) have several maxima and minima within the energy range studied. Fig. 4(a) shows that the absorptions start with zero photon energy indicating that the materials have no band gap between valence and conduction bands, *e.g.*, metallic nature. All the spectra rapidly decrease to zero at ~ 26 eV. We also observed that the photoconductivity (Fig. 4 (b)) starts with zero photon energy indicating metallic nature of the materials. The results of the absorption and conductivity are in agreement with the band structure results.

Fig. 4 (c) shows the reflectivity spectra of ANNi₃ (A = Pt, Ag, Pd and Zn). We notice that the reflectivity is $\sim 0.58 - 0.86$ in the infrared region and the value drops in the high energy region with some peaks as a result of interband transition. PtNNi₃ and PdNNi₃ have relatively larger reflectivity compared to that of ZnNNi₃. The large reflectivity in very low energy range indicates the characteristics of high conductance in the low energy region.

Besides, the electron energy loss function is also an important optical parameter describing the energy loss of a fast electron traversing a certain material, and the peaks in loss-function spectra represent the characteristics associated with the plasma resonance. In addition, the positions of peaks in spectra, which correspond to the so-called plasma frequency, point out the transition from the metallic property [$\epsilon_1(\omega) < 0$] to the dielectric property [$\epsilon_1(\omega) > 0$] for a material. Moreover, the peaks of loss function correspond to the trailing edges in the reflection spectra.

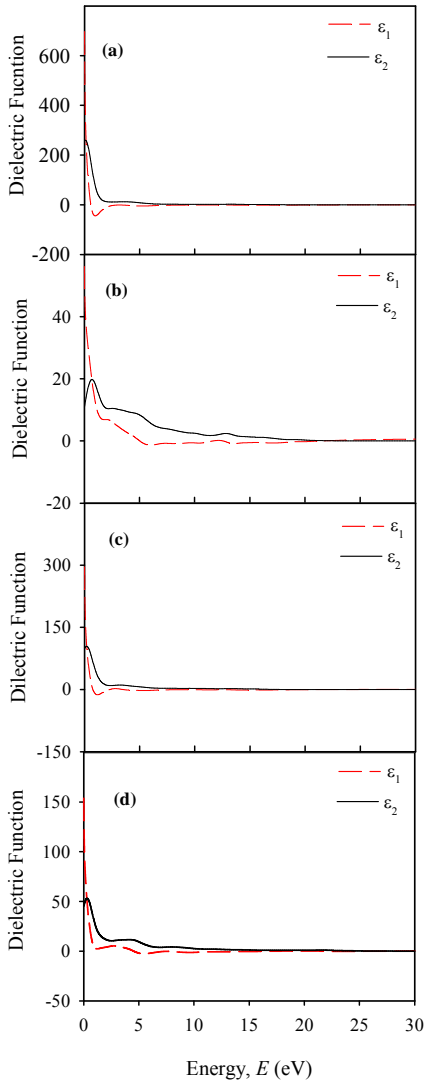


Fig. 3. The dielectric function of (a) AgNNi_3 , (b) PdNNi_3 , (c) PtNNi_3 and (d) MgCNi_3 .

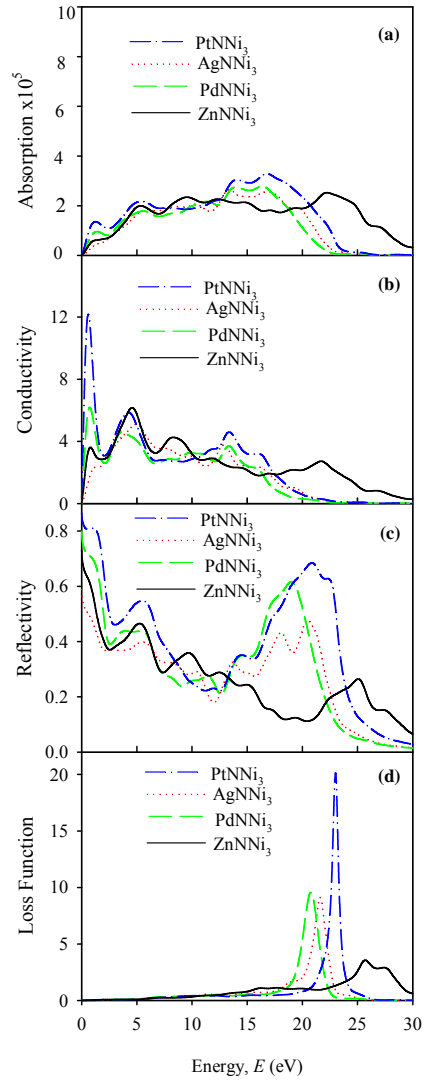


Fig. 4. The (a) absorption, (b) conductivity, (c) reflectivity and (d) loss function of PtNNi_3 , AgNNi_3 , PdNNi_3 and ZnNNi_3 .

4. Conclusion

We studied the structural, elastic, electronic and optical properties of three predicted ANNi_3 ($A = \text{Pt}, \text{Ag}, \text{Pd}$) in comparison with the isostructural superconducting ZnNNi_3 . The calculated elastic constants satisfy the traditional mechanical stability conditions for the considered structures. The band structures of all phases show metallic nature in which

the $3d$ states of transition metal atoms play dominant roles near the Fermi levels just like the superconductor $ZnNi_3$. The three compounds studied are less likely to show superconductivity. Finally, the dielectric function, absorption spectrum, conductivity, reflectivity and energy-loss spectrum have been calculated and discussed in detail. The reflectance spectra show that these materials have the potential to be used in the solar cell to remove solar heating.

Reference

1. J. B. Goodenough and J. M. Longo, Magnetic and other properties of oxides and related compounds, in: K.-H. Hellwege, O. Madelung (Eds.), Landolt-Bornstein, New Series, Group III, vol. 4a, Springer-Verlag, Berlin, 1970.
2. M. Y. Chern, D. A. Vennos, and F. J. DiSalvo, *J. Solid State Chem.* **96**, 415 (1992). [http://dx.doi.org/10.1016/S0022-4596\(05\)80276-2](http://dx.doi.org/10.1016/S0022-4596(05)80276-2)
3. J. Jäger, D. Stahl, P. C. Schmidt, and R. Knipf, *Angew. Chem.* **105**, 738 (1993). <http://dx.doi.org/10.1002/ange.19931050512>
4. T. He, Q. Huang, A. P. Ramirez, Y. Wang, K. A. Regan, N. Rogado, M. A. Hayward, M. K. Haas, J. S. Slusky, K. Inumaru, H. W. Zandbergen, N. P. Ong, and R. J. Cava, *Nature (London)* **411**, 54 (2001). <http://dx.doi.org/10.1038/35075014>
5. M. Uehara, A. Uehara, K. Kozawa, and Y. Kimishima, *J. Phys. Soc. Japan* **78**, 033702 (2009). <http://dx.doi.org/10.1143/JPSJ.78.033702>
6. I. R. Shein, V. V. Bannikov, and A. L. Ivanovskii, *Phys. Status Solidi B* **247**, 72 (2010). <http://dx.doi.org/10.1002/pssb.200945216>
7. W. H. Cao, B. Hea, C. Z. Liao, L. H. Yang, L. M. Zeng, and C. Dong, *J. Solid State Chem.* **182**, 3353 (2009). <http://dx.doi.org/10.1016/j.jssc.2009.10.002>
8. Z. F. Hou, *Solid States Commun.* **150**, 1874 (2010). <http://dx.doi.org/10.1016/j.ssc.2010.07.047>
9. M. Tütüncü and G. P. Srivastava, *J. Phys.: Condens. Matter* **18**, 11089. (2006). <http://dx.doi.org/10.1088/0953-8984/18/49/004>
10. A. B. Karki, Y. M. Xiong, D. P. Young, and P. W. Adams, *Phys. Rev. B* **79**, 212508 (2009). <http://dx.doi.org/10.1103/PhysRevB.79.212508>
11. M. Uehara, A. Uehara, K. Kozawa, T. Yamazaki, and Y. Kimishima, *Physica C* **470**, S688 (2009). <http://dx.doi.org/10.1016/j.physc.2009.11.131>
12. C. Li, W. G. Chen, F. Wang, S. F. Li, Q. Sun, S. Wang, and Y. Jia, *J. Appl. Phys.* **105**, 123921 (2009). <http://dx.doi.org/10.1063/1.3156641>
13. C. M. I. Okoye, *Physica B* **405**, 1562 (2010). <http://dx.doi.org/10.1016/j.physb.2009.12.040>
14. V. V. Bannikov, I. R. Shein, and A. L. Ivanovskii, *Comput. Mater. Sci.* **49**, 457 (2010). <http://dx.doi.org/10.1016/j.commatsci.2010.05.036>
15. J. H. Shim, S. K. Kwon, and B. I. Min, *Phys. Rev. B* **64**, 180510 (2001). <http://dx.doi.org/10.1103/PhysRevB.64.180510>
16. K. S. Alexandrov and B. V. Beznosikov, *Perovskites: Present and Future*, Novosibirsk, pp. 200-201 (2004) [in Russian].
17. V. V. Bannikov, I. R. Shein, and A. L. Ivanovskii, *Physica B* **405**, 4615 (2010). <http://dx.doi.org/10.1016/j.physb.2010.08.046>
18. M. A. Helal and A. K. M. A. Islam, *Physica B* **406**, 4564 (2011). <http://dx.doi.org/10.1016/j.physb.2011.09.018>
19. M. C. Payne, M. P. Teter, D. C. Allan, T. A. Arias, and J. D. Joannopoulos, *Rev. Mod. Phys.* **64**, 1045 (1992). <http://dx.doi.org/10.1103/RevModPhys.64.1045>
20. J. P. Perdew, S. Burke, and M. Ernzerhof, *Phys. Rev. Lett.* **77**, 3865 (1996). <http://dx.doi.org/10.1103/PhysRevLett.77.3865>
21. M. Segall, P. Lindan, M. Probert, C. Pickard, P. Hasnip, S. Clark, and M. Payne, *J. Phys.: Condens. Matter.* **14**, 271 (2002). <http://dx.doi.org/10.1088/0953-8984/14/2/313>

22. H. J. Monkhorst and J. Pack, Phys. Rev. **13**, 5188 (1976).
<http://dx.doi.org/10.1103/PhysRevB.13.5188>
23. B. G. Pfrommer, M. Coote, S. G. Louie, and M. L. Cohen, J. Comp. Phys. **131**, 33 (1997).
<http://dx.doi.org/10.1006/jcph.1996.5612>
24. G. Grimvall, Thermophysical Properties of Materials (North-Holland, Amsterdam, 1986).
25. A. Bouhemadou, Braz. J. Phys. **40**, 52 (2010).
<http://dx.doi.org/10.1590/S0103-97332010000100009>
26. R. Hill, Proc. Phys. Soc. London **65**, 350 (1952).
27. M. V. Nevitt, S. Chan, J. Z. Liu, M. H. Grinsditch, and Y. Fang, Physica B **152**, 231 (1988).
[http://dx.doi.org/10.1016/0921-4534\(88\)90133-5](http://dx.doi.org/10.1016/0921-4534(88)90133-5)
28. C. Zener; Elasticity and Anelasticity of Metals, University of Chicago, Chicago, (1948).
29. J. Haines, J. Leger, and G. Bocquillon, Ann. Rev. Mater. Res. **31**, 1 (2001).
<http://dx.doi.org/10.1146/annurev.matsci.31.1.1>
30. S. F. Pugh, Philos. Mag. **45**, 823 (1954).
31. W. L. McMillan, Phys. Rev. **167**, 331 (1968). <http://dx.doi.org/10.1103/PhysRev.167.331>
32. M. Rajagopalan, P. Selvamani, G. Vaitheeswaran, V. Kanchana, and M. Sundareswari, Solid State Commun. **120**, 215 (2001). [http://dx.doi.org/10.1016/S0038-1098\(01\)00360-X](http://dx.doi.org/10.1016/S0038-1098(01)00360-X)